Scaling behavior in explosive fragmentation

A. Diehl,[1] H. A. Carmona,[2] L. E. Araripe,[1] J. S. Andrade, Jr.,[1,3] and G. A. Farias[1]
[1]*Departamento de Física, Universidade Federal do Ceará, 60451-970 Fortaleza, Ceará, Brazil*
[2]*Departamento de Física e Química, Universidade Estadual do Ceará, 60740-000 Fortaleza, Ceará, Brazil*
[3]*PMMH-ESPCI, 10 rue Vauquelin, 75231 Paris Cedex 05, France*
(Received 8 June 2000)

We investigate the explosive fragmentation process in two dimensions using molecular-dynamics simulations. We show that the mass distribution of fragments follows a power law, with a scaling exponent that is strongly dependent on the macroscopic characteristics of the system prior to the explosion process. In particular, for thermalized initial configurations at low temperatures, we observe that the exponent is close to -1. We suggest that this result can be interpreted in terms of a multiplicative fracture process.

PACS number(s): 46.50.+a, 64.60.Ak

I. INTRODUCTION

The fragmentation process is ubiquitous in everyday life. From practical experience, we know that an object under stress or shock will break up into smaller pieces. Although complex under a microscopic point of view, some remarkable statistical features can be observed. The form of the mass distribution of fragments, for example, has received a lot of attention in recent years. Experiments on impact fragmentation using glass spheres show that the mass distribution follows a power law, with an exponent $-\frac{2}{3}$ [1]. Ishii and Matsushita [2] have studied the fragment size and mass distribution of long, thin glass rods and found that they change from a log-normal to a power-law form as the falling height is increased. Oddershede *et al*. [3] observed a power-law distribution in experiments of impact fragmentation using different materials (e.g., gypsum, soap, and stearic) of different shapes (e.g., balls, cubes, plates, and bars). The scaling exponent was found to be rather dependent on the shape of the object, but insensitive to the type of material. This exponent independence was then interpreted as an evidence that fragmentation can be a self-organized critical phenomena [4]. Using thick plates of dry clay, Meibom and Balslev [5] observed that the mass distribution of fragments displays a crossover between two different power-law regimes for fragments larger and smaller than the plate thickness. Finally, power-law behavior has also been observed in *sandwich* experiments using thin glass and plaster plates, but the exponent, once more, was shown to be nonuniversal with the input energy [6].

The foregoing experimental observations about the fragmentation process induced many theoretical studies. The simplest one, based on an one-dimensional process [2,7], predicts a log-normal distribution. More realistic models, using assumptions about preexisting flaws and breaking mechanisms, yield power-law behavior [8,9]. Incorporating hierarchical order to the process in a probabilistic type of model, Marsili and Zhang [10] could predict a nonuniversal power-law behavior for fragmentation, with an exponent that is dependent on its detailed breaking mechanism and initial conditions. These models, however, are not able to reproduce the nonuniversal behavior observed in experiments.

The numerical modeling of the fragmentation process represents today an important tool for the understanding of the microscopic mechanisms governing this physical phenomenon. For example, Hayakawa [11] observed power-law behavior modeling a three-dimensional fractured object by a set of mass points connected by elastic springs. Inaoka *et al*. [12] modeled a fracture in terms of a competitive process taking place during the crack propagation. The resulting power-law behavior followed by a flat tail in the cumulative distribution of mass fragments is consistent with the experimental observations of Meibom and Balslev [5].

Recently, Ching *et al.* [13] studied fragmentation using a molecular-dynamics (MD) approach similar to the one introduced by Holian and Grady [14]. The fragmented object is represented as a set of particles interacting via the Lennard-Jones (LJ) potential, while the fracture process develops due to random initial velocities assigned to the particles. The resulting steady-state cumulative mass distribution has an effective power-law region, with an exponent that increases with the initial energy assigned to the particles. Ching *et al.* interpreted this dependence in the exponent as an indication that fragmentation is not a self-organizing phenomenon, contrary to the assumption of Oddershede *et al.* [3].

The question of criticality in fragmentation, however, is far from being completely answered. Very recently, it has been suggested that, in impact fragmentation, criticality could be tuned at a nonzero impact energy [15,16], so that the fragment-size distribution should satisfy a scaling form similar to that of the cluster-size distribution of percolation clusters, but belonging to another universality class [17]. In the present paper, we investigate the explosive fragmentation process using classical MD simulations. We study the mass distribution of fragments focusing on the dependence of the scaling exponent with the external input energy provided to ''explode'' a given object. Contrary to the observations made in Ching's *et al.* experiment [13], we show that the fragment mass distribution displays power-law behavior, with a scaling exponent that is independent of the input energy. Our simulations indicate, however, that this exponent is sensitive to the way in which the object to be fragmented is prepared, i.e., to the initial configuration of the system. The structure of this paper is the following. The model for fragmentation and the simulation details are described in Sec. II. In Sec. III, we present and discuss our results and the con-

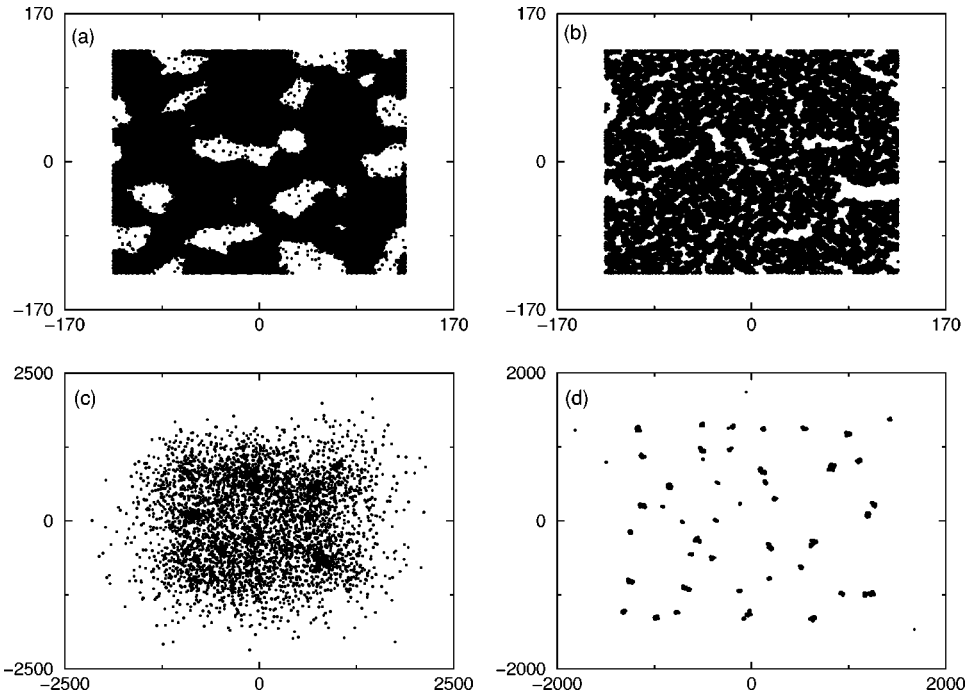

FIG. 1. Snapshots of the initial state representing the object to be fragmented, in a thermalized configuration, at a reduced temperature (a) $T^*=\kappa T/\epsilon=0.37$ and (b) $T^*=0.037$. In (c) and (d), we show the resulting fragmented states of (a) and (b), respectively, after 150 000 MD time steps and using $R=0.43$ for both cases. The number density is $\rho\sigma^2=0.61$ in all cases and the number of particles is fixed to $N=40\,000$. The xy coordinates are in LJ units.

clusions are summarized in Sec. IV.

II. MODEL

In order to model the fragmentation process, we start by describing the system to be fragmented. For the sake of comparison with previous studies [13], we build up an object in two different ways. In the *random* initial configuration case, we just place the particles randomly in the MD simulation box, according to the desired number density, and the particle's velocities are settled in random directions. In the second case, we use MD simulation to generate a *thermalized* configuration as an initial state of the system. The particles interact through a $6-12$ LJ pair potential and the system is brought to the desired equilibrium temperature, using the neighbor-list method with periodic boundary conditions in all directions. This allows us to simulate as much as 40 000 particles with a 300 MHz Pentium II PC.

In Figs. 1(a) and 1(b) we show snapshots of the initial thermalized configurations for a two-dimensional object with 40 000 particles and number density $\rho^*=\rho\sigma^2=0.61$. In Fig. 1(a) the reduced temperature is $T^*=\kappa T/\epsilon=0.37$, while in case (b) the temperature is $T^*=0.037$. Here, σ and ϵ are the LJ distance and energy units, respectively. The positions and velocities obtained with these processes are then used as initial states in the fragmentation process.

To simulate the expansion process that follows an explosive event, one can add an isotropic term to the initial velocities, as follows [13–15]:

$$\boldsymbol{v}_i(0)=\boldsymbol{v}_i^T+C\boldsymbol{r}_i(0), \tag{1}$$

where $\boldsymbol{v}_i^T$ are the initial velocities and $\boldsymbol{r}_i(0)$ are the initial positions, obtained in the previous (randomic or thermalized) stage. The proportionality constant C (with units of inverse of time) is a measure of the initial energy imparted to the object. From time zero onward, no energy is added to the system and the particles positions and velocities are obtained by solving Newton's equations of motion with *free boundary conditions*, different from the expanding boundary conditions used by Holian and Grady [14]. It is useful to introduce here the parameter R, the ratio between the initial (total) kinetic energy to the initial potential energy, immediately after the velocities are settled according to Eq. (1). As a result, the system expands and the particles distribute themselves in clusters (or fragments) of different masses [see Figs. 1(c) and 1(d)].

In order to generate good statistics, we adapted the neighbor-list method [18] to account for the free boundary conditions in the fragmentation process. Basically, at time zero, we use a simulation box larger then the one used for building the object. This is our fragmentation space. This large simulation box is divided into cells, in the usual manner of the neighbor-list method, but without introducing periodic boundary conditions. At each step, we check if there is a particle crossing the boundary of the simulation box. If that is the case, we rescale the size of the box and rebuild the neighbor list. To update the particle's coordinates and velocities, we use the leapfrog integration technique [18] with a time step $\Delta t=0.005$, which is sufficiently small to ensure global energy conservation.

Next, we perform the cluster (or fragment) identification and counting. Each particle is considered as a monomeric cluster with unitary mass. Two particles will belong to the same cluster if they are separated by a distance smaller than an arbitrary cutoff, $r_c=3\sigma$. The fragments are classified according to their mass m and counted to compute the distribution $n(m)$, normalized here by the total number of fragments. As $n(m)$ is not a continuous function, it is more convenient to work with the cumulative distribution [3], the total number of fragments with masses larger than or equal to m, defined as

$$F(m)=\frac{1}{m}\int_m^\infty n(m')dm'. \tag{2}$$

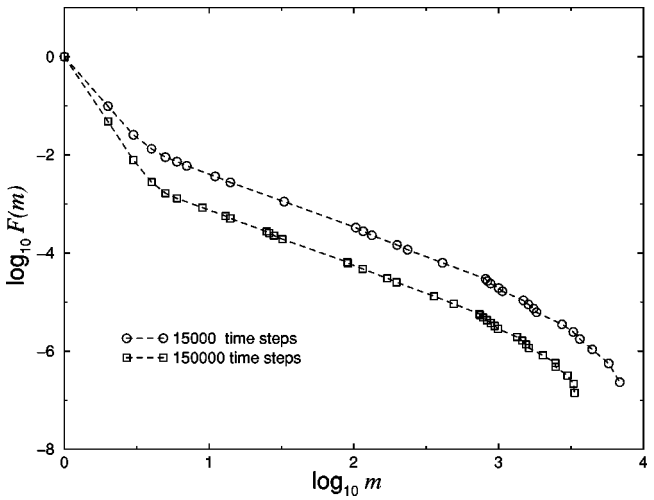

FIG. 2. Double logarithmic plot of the cumulative mass distribution of fragments $F(m)$ after 15 000 (circles) and 150 000 (squares) MD time steps. Although the object is free to expand indefinitely, the fragment mass distribution at the intermediate mass region becomes steady after a sufficient number of time steps. The parameters used in this simulation are the same as those used in Fig. 1(a).

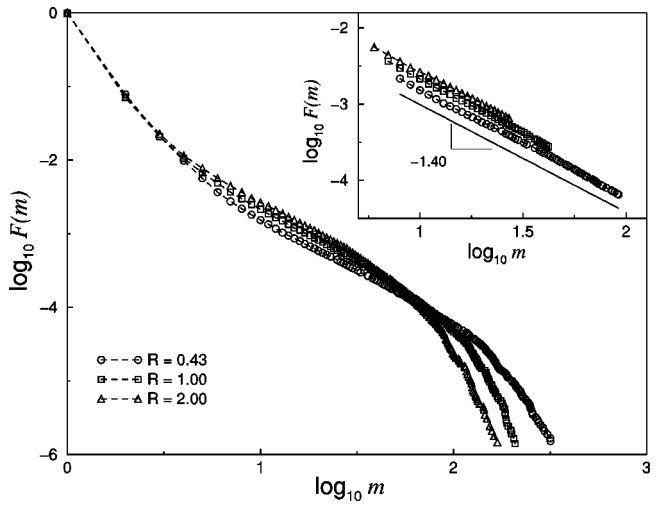

FIG. 3. Double logarithmic plot of the cumulative mass distribution of fragments $F(m)$ after 150 000 time steps, at different values of R, obtained from an initial random configuration as shown in Ref. [13]. A power law is observed for an intermediate range of mass values, with an exponent $\beta = 1.40 \pm 0.02$ independently of R. For large m, the distributions decay exponentially. The solid line in the inset is the least-square fit to the data in the scaling regions for all cases, with the number indicating the exponent β. The number of particles is fixed to $N = 40\,000$.

As in Ref. [3], if $n(m)$ follows a power law, $n(m) \propto m^{-\beta}$, $F(m)$ should also exhibit scaling with the same exponent β. As shown in Fig. 2, although the system is free to expand, the cumulative distribution $F(m)$ becomes steady after a sufficient number of time steps. In our simulations, we only calculate $F(m)$ after 150 000 time steps.

III. RESULTS AND DISCUSSION

For the sake of comparison with previous results (see Ref. [13]), we first present results obtained with random initial configurations. The number density is $\rho^* = 0.61$ and $N = 40\,000$ particles. In Fig. 3 we plot the distribution $F(m)$ against the fragment mass m for different values of the parameter R. A power-law region can be observed for intermediate masses, with an exponent $\beta = 1.40 \pm 0.02$ for all cases. For large m, the distributions fall off exponentially. Clearly, the exponent β is unchanged when the parameter R (a measure of the input energy) is increased from 0.43 to 2.00. The width of the region for which the power law holds also becomes narrower as R increases. It is the definition of the range of fragment masses for which the power law holds that gives the larger source of error to the exponent β. Although the value of the exponent β that we found is in agreement with the results obtained by Ching *et al.* [13], namely, $\beta - 1 = 0.41$ for $R = 0.43$, we did not observe the energy dependence detected in their study. This can perhaps be attributed to the small number of particles used in Ref. [13], typically $N = 4200$.

Next we discuss the results of simulations performed with thermalized states as initial configurations for the fragmentation process. In Fig. 4 the equilibrium temperature is $T^* = 0.37$, while the number density and the range of R values are the same as in Fig. 3. Again we observe a power-law region for intermediate masses, but now with an exponent $\beta = 1.14 \pm 0.03$. The range of this scaling region is larger than that in Fig. 3, extending over almost two orders of magnitude for $R = 0.43$ and decreasing upon increasing R, as the formation of large clusters becomes less probable with large energy inputs. Analyzing the radial distribution function $g(r)$ for the initial configuration used in Fig. 4 we found that the system is a mix solid-liquid phase.

In order to simulate the fragmentation of a solid, we decrease the initial configuration temperature to $T^* = 0.037$, maintaining the number density $\rho^* = 0.61$. In Fig. 5 we show the steady state $F(m)$ for a range of R values between 0.43 and 2.00. Once again, we can identify a region of masses

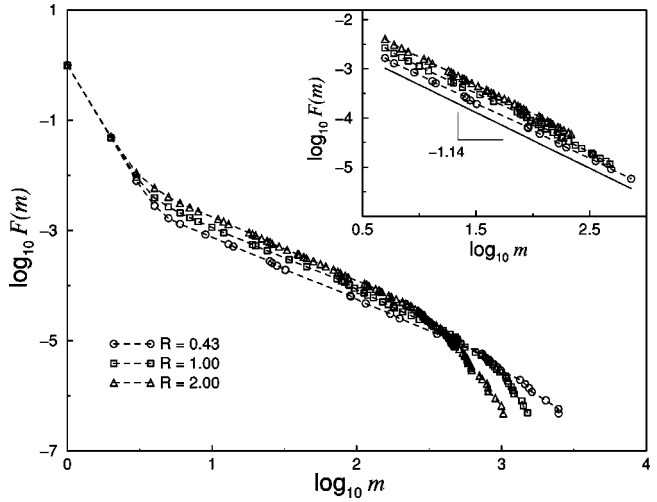

FIG. 4. Cumulative mass distribution for a thermalized initial configuration at $T^* = 0.37$ [see Fig. 1(a)], for the same values of R and N used in Fig. 3. The power-law region is wider than that obtained if Fig. 3 for the same R, but now the scaling exponent is $\beta = 1.14 \pm 0.03$, as shown in the inset.

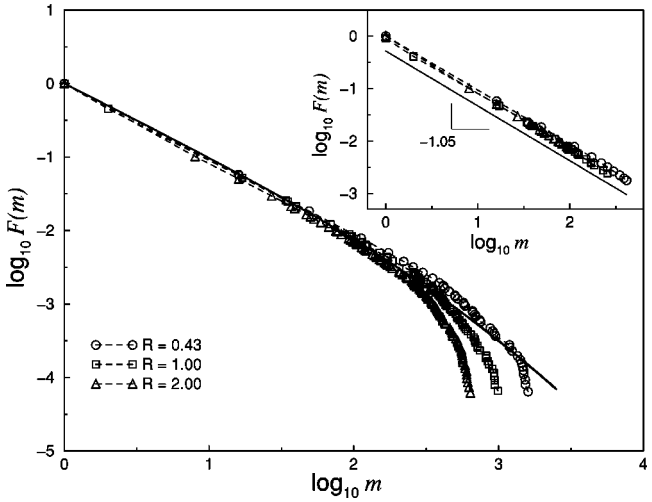

FIG. 5. Cumulative mass distribution for the thermalized initial configuration shown in Fig. 1(b) ($T^*=0.037$). The solid line corresponds to the cumulative form $F(m)$ of the log-normal distribution [Eq. (3)], with $\log \overline{m}=5.9$ and $\sigma^2=4.0$. According to the solid line shown in the inset, a power law with an exponent $\beta=1.05\pm0.02$ represents the least-square fit to the data in the scaling region.

where $F(m)$ follows a power-law behavior, with an exponent $\beta=1.05\pm0.02$, which remains approximately unchanged within the range of R values used in the simulations. It is important to mention that several test simulations we carried out with objects that are different, but prepared in the same way (e.g., two objects thermalized at $T^*=0.037$), showed the same power-law exponent.

The different values of R used to generate Figs. 2–5 are reached by increasing the value of the constant C in Eq. (1). We observe that the exponent β is rather robust to changes in the input energy. On the other hand, our results indicate that β is sensitive to the way in which the object to be fragmented is prepared, that is, to the initial state of the system. Indeed, when comparing the curves for $R=0.43$ obtained with different initial configurations, we see that the power-law exponent varies from $\beta=1.40$ (Fig. 3) to 1.05 (Fig. 5). Therefore, we suggest that this exponent should solely depend on the *macroscopic* properties of the object. For instance, as the initial configuration resembles more closely a solid state, the exponent β tends to a value close to 1.0. Additional simulations performed with a number density $\rho^*=0.95$ and a reduced temperature $T^*=0.37$ (a typical two-dimensional LJ solid) produced a power-law exponent of $\beta=1.07\pm0.02$.

It is possible to interpret the origin of the $1/m$ type of distribution that we found for thermalized initial configurations at low temperatures, in terms of a typical *multiplicative process* [19]. In the solid phase, the fragments form rapidly as one gives kinetic energy to the system. In this situation, the system has enough potential energy to hold clusters together. A small fragment with mass M_n is produced from a large one with mass M_0 through a succession of N breaks, such that the difference $M_{n-1}-M_n$ is a random portion of the fragment with mass M_{n-1}. If we apply the central limit theorem [19], and assume that every fragmentation of a cluster produces the same fractional increase to the distribution of fragment masses, it results that $n(m)$ should follow a log-normal distribution,

$$n(m)=\frac{1}{m\sqrt{2\pi\sigma^2}}\exp\left[\frac{-(\log m-\log \overline{m})^2}{2\sigma^2}\right], \tag{3}$$

where

$$\log \overline{m}=\int_0^\infty n(m)\log m\,dm \quad \text{and} \quad \sigma^2=\overline{(\log m)^2}-(\log \overline{m})^2. \tag{4}$$

If σ^2 is sufficiently large, only the $1/m$ term remains for small masses. In our case, σ^2 can be quite large; for example, $\sigma^2=4.0$ and $\log \overline{m}=5.9$ for a run with 40 000 particles at $T^*=0.037$ and $R=0.43$. As shown in Fig. 5, the log-normal expression for $F(m)$ with these parameters fits well the results from numerical simulations. Therefore, it provides a plausible mechanism to explain the power-law behavior that we observe at low temperatures and in the range of small masses. Corrections to the $1/m$ distribution at large masses are due to the finite size of the system.

For liquids, the fragmentation process is slower than for solids. Besides, there will be particles that do not belong to any cluster and eventually form other clusters, or adhere to an existing fragment, increasing its mass. In both cases, the amplification process may lead to a power-law distribution with a coefficient different from -1 [19].

IV. CONCLUSIONS

In summary, we have presented in this paper a model for two-dimensional explosive fragmentation using molecular-dynamics simulation. The essential features of the fragmentation process of an object composed by a set of Lennard-Jones particles are shown to be a result of the competition between the input kinetic energy imparted to the system and the cohesive forces that maintain its integrity prior to the explosion. Our simulations predict that the mass distribution of fragments should display power-law behavior, with an exponent that is independent of the input energy representing the explosion process. We show that, for an initial configuration resembling a solid, the fragment mass distribution follows an $1/m$ behavior, consistent with a typical multiplicative process [19].

How realistic is the fragmentation model used in our simulations? For a solid object, like the one shown in Fig. 1(b), the observed scaling exponent corresponding to small masses is similar to that observed in experiments with gypsum disks [3]. However, the exponential crossover that we observed for larger fragment masses cannot be attributed to the morphology of the object being fragmented, as in Ref. [3]. In our case, the crossover should be related to finite size and input energy effects, both limiting the largest fragment mass.

It has recently been suggested that the crossover mass (or the largest fragment mass) can be used as the order parameter defining the critical region of fragmentation [16,17]. The scaling exponent found in these studies is exactly one-half of

the correlation length exponent for two-dimensional percolation clusters [17]. It appears that the results of our simulations, however, have no direct analogy with percolation theory. To elucidate the dependence of the exponential crossover on the energy input found in our results, additional simulations with larger systems and at several different conditions are needed.

ACKNOWLEDGMENTS

This work was supported by the Brazilian funding agencies CNPq—Conselho Nacional de Desenvolvimento Científico e Tecnológico and FUNCAP—Fundação Cearense de Amparo à Pesquisa. L.E.A. greatly appreciates the support of the PIBIC/CNPq program.

[1] J.J. Gilvarry and B.H. Bergstrom, J. Appl. Phys. **32**, 400 (1961).
[2] T. Ishii and M. Matsushita, J. Phys. Soc. Jpn. **61**, 3474 (1992).
[3] L. Oddershede, P. Dimon, and J. Bohr, Phys. Rev. Lett. **71**, 3107 (1993).
[4] P. Bak, C. Tang, and K. Wiesenfeld, Phys. Rev. Lett. **59**, 381 (1987).
[5] A. Meibom and I. Balslev, Phys. Rev. Lett. **76**, 2492 (1996).
[6] T. Kadono, Phys. Rev. Lett. **78**, 1444 (1997).
[7] M. Matsushita and K. Sumida, Chuo Univ. **31**, 69 (1981).
[8] D.L. Turcotte, J. Geophys. Res. **91**, 1921 (1986).
[9] S. Redner, in *Statistical Models for the Fracture of Disorder Media*, edited by H.J. Hermann and S. Roux, Random Material and Processes Series (Elsevier Science, New York, 1990).
[10] M. Marsili and Y.-C. Zhang, Phys. Rev. Lett. **77**, 3577 (1996).
[11] Y. Hayakawa, Phys. Rev. B **53**, 14 828 (1996).
[12] H. Inaoka, E. Toyosawa, and H. Takayasu, Phys. Rev. Lett. **78**, 3455 (1997).
[13] E.S.C. Ching, Y.Y. Yiu, and K.F. Lo, Physica A **265**, 119 (1999).
[14] B.L. Holian and D.E. Grady, Phys. Rev. Lett. **60**, 1355 (1988).
[15] Wm.T. Ashurst and B.L. Holian, Phys. Rev. E **59**, 6742 (1999).
[16] F. Kun and H.J. Herrmann, Phys. Rev. E **59**, 2623 (1999).
[17] J.A. Astrom, B.L. Holian, and J. Timonen, Phys. Rev. Lett. **84**, 3061 (2000).
[18] D.C. Rapaport, *The Art of Molecular Dynamics Simulation* (Cambridge University Press, Cambridge, 1996).
[19] B.J. West and M.F. Shlesinger, Int. J. Mod. Phys. B **3**, 795 (1989).